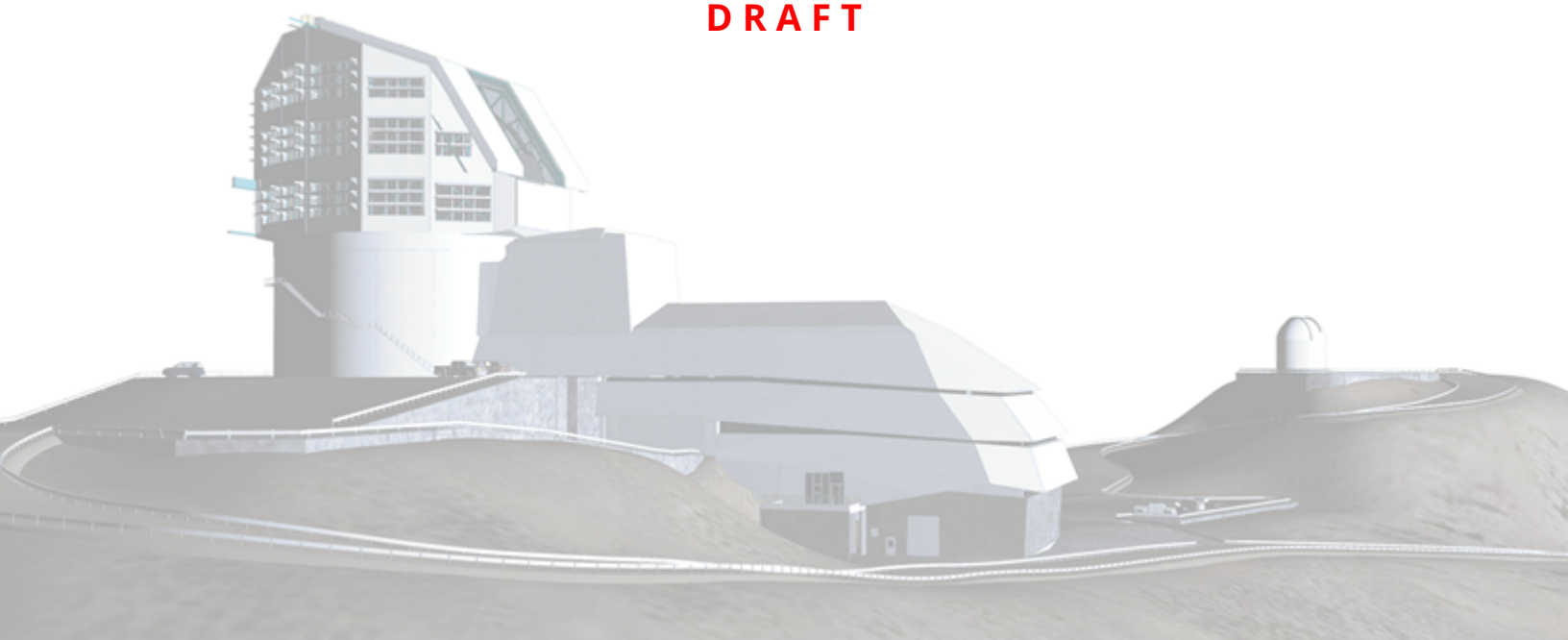

Vera C. Rubin Observatory
Systems Engineering

An Interim Report on the ComCam On-Sky Campaign

Many authors

SITCOMTN-149

Latest Revision: 2024-12-03

DRAFT

Abstract

A summary of what we have learned from the initial period of ComCam observing

Change Record

Version	Date	Description	Owner name
1	YYYY-MM-DD	Unreleased.	Robert Lupton

Document source location: `https://github.com/lsst-sitcom/sitcomtn-149`

Contents

An Interim Report on the ComCam On-Sky Campaign

1 Introduction

The Vera C. Rubin Observatory on-sky commissioning campaign using the Commissioning Camera (ComCam) began on 24 October 2024 and is forecasted to continue through mid-December 2024. This interim report provides a concise summary of our understanding of the integrated system performance based tests and analyses conducted during the first weeks of the ComCam on-sky campaign. The emphasis is distilling and communicating what we have learned about the system. The report is organized into sections to describe major activities during the campaign, as well as multiple aspects of the demonstrated system and science performance.

Warning: Preliminary Results

All of the results presented here are to be understood as work in progress using engineering data. It is expected at this stage, in the middle of on-sky commissioning, that much of the discussion will concern open questions, issues, and anomalies that are actively being worked by the team. Additional documentation will be provided as our understanding of the demonstrated performance of the as-built system progresses.

1.1 Charge

We identify the following high-level goals for the interim report:

- **Rehearse workflows for collaboratively developing documentation** to describe our current understanding of the integrated system performance, e.g., to support the development of planned Construction Papers and release documentation to support the Early Science Program [RTN-011]. This report represents an opportunity to collectively exercise the practical aspects of developing documentation in compliance with the policies and guidelines for information sharing during commissioning [SITCOMTN-076].
- **Synthesize the new knowledge** gained from the ComCam on-sky commissioning cam-

paign to inform the optimization of activities between the conclusion of the ComCam campaign and the start of the on-sky campaign with the LSST Camera (LSSTCam).

- **Inform the Rubin Science Community** on the progress of the on-sky commissioning campaign using ComCam.

Other planned systems engineering activities will specifically address system-level verification ([LSE-29] and [LSE-30]) using tests and analysis from the ComCam campaign. While the analyses in this report will likely overlap with the generation of verification artifacts for systems engineering, and system-level requirement specifications will serve as key performance benchmarks for interpreting the progress to date, formal acceptance testing is not an explicit goal of this report.

The groups within the Rubin Observatory project working on each of the activities and performance analyses are charged with contributing to the relevant sections of the report. The anticipated level of detail for the sections ranges from a paragraph up to a page or two of text, depending on the current state of understanding, with **quantitative performance** expressed as summary statistics, tables, and/or figures. The objective for this document is to **summarize the state of knowledge of the system**, rather than how we got there or "lessons learned". The sections refer to additional supporting documentation, e.g., analysis notebooks, other technotes with further detail, as needed. Given the timelines for commissioning various aspects of the system, it is natural that some sections will have more detail than others.

The anticipated milestones for developing this interim report are as follows:

- 18 Nov 2024: Define charge
- 4 Dec 2024: First drafts of report sections made available for internal review
- 11 Dec 2024: Revised drafts of report sections made available for internal review; editing for consistency and coherency throughout the report
- 18 Dec 2024: Initial version of report is released

Warning: On-sky Pixel Image Embargo

All pixel images and representations of pixel images of any size field of view, including individual visit images, coadd images, and difference images based on ComCam commissioning on-sky observations must be kept internal to the Rubin Observatory Project team, and in particular, cannot be included in this report. Embargoed pixel images can only be referenced as authenticated links. See [SITCOMTN-076] for details.

2 System Performance Analysis

3 Active Optics System Commissioning

4 Image Quality

5 Data Production

6 Calibration Data

7 Science Pipelines Commissioning Observations

8 Throughput for Focused Light

9 Delivered Image Quality and PSF

10 Instrument Signature Removal

The quality of the instrument signal removal (ISR) has improved during commissioning, as we create and deploy updated calibration products that better represent the LSSTComCam system. The following discussion summarizes our current understanding of a variety of features,

both expected and newly seen on LSSTComCam, and presents our expected prognosis of the behavior of the full LSSTCam.

10.1 Phosphorescence

There are regions on some of the detectors (most visible in R22_S01, detector=1) which show bright emission, particularly at bluer wavelengths, as shown in Figure 1. This is believed to be caused by a thin layer of remnant photo-resist from the manufacturing process that remained on the detector surface, and is now permanent due to the subsequent addition of the anti-reflective coating. In addition to the large areas, there are also discrete point-source-like or cosmic-ray-like defects caused by accumulations of this material. Adding to the difficulty of mitigating these defects is that this photo-resist is known to be phosphorescent, explaining why these regions are more noticeable in the bluer filters.

The initial studies of this show that these features can continue to emit light up to several minutes after they've been illuminated. Due to the long duration of these features, we decided to place manual defect masks over the worst regions. The first of these manual masks takes up about 3.5% of that detector, smaller than but consistent with estimates that this would create a pixel loss of approximately one amplifier.

The ITL detectors in LSSTCam are believed to have been cleaned better, so this should be less of an issue on the full camera.

10.2 Vampire pixels

There are defects on LSSTComCam that have been classified as "vampire" pixels, as they appear as a bright defect with a (generally) axisymmetric region surrounding the bright core, as if the defect is draining charge from its neighbors. The naming is at least broadly correct, as integrating to large radii shows that these regions do appear to conserve charge. There is an intensity dependence that makes these vampire pixels different than standard hot pixels, as these pixels do not show up on dark frames, only on flats and science exposures, where the detector surface is illuminated. After the initial discovery of the bright obvious vampires, we added new masking code that identifies the bright cores that are above 2.0 on the combined flat (pixels that are greater than 200% of the median flat level), and adds circular masks to the defect list. This appears to find the most problematic examples, but as we have improved

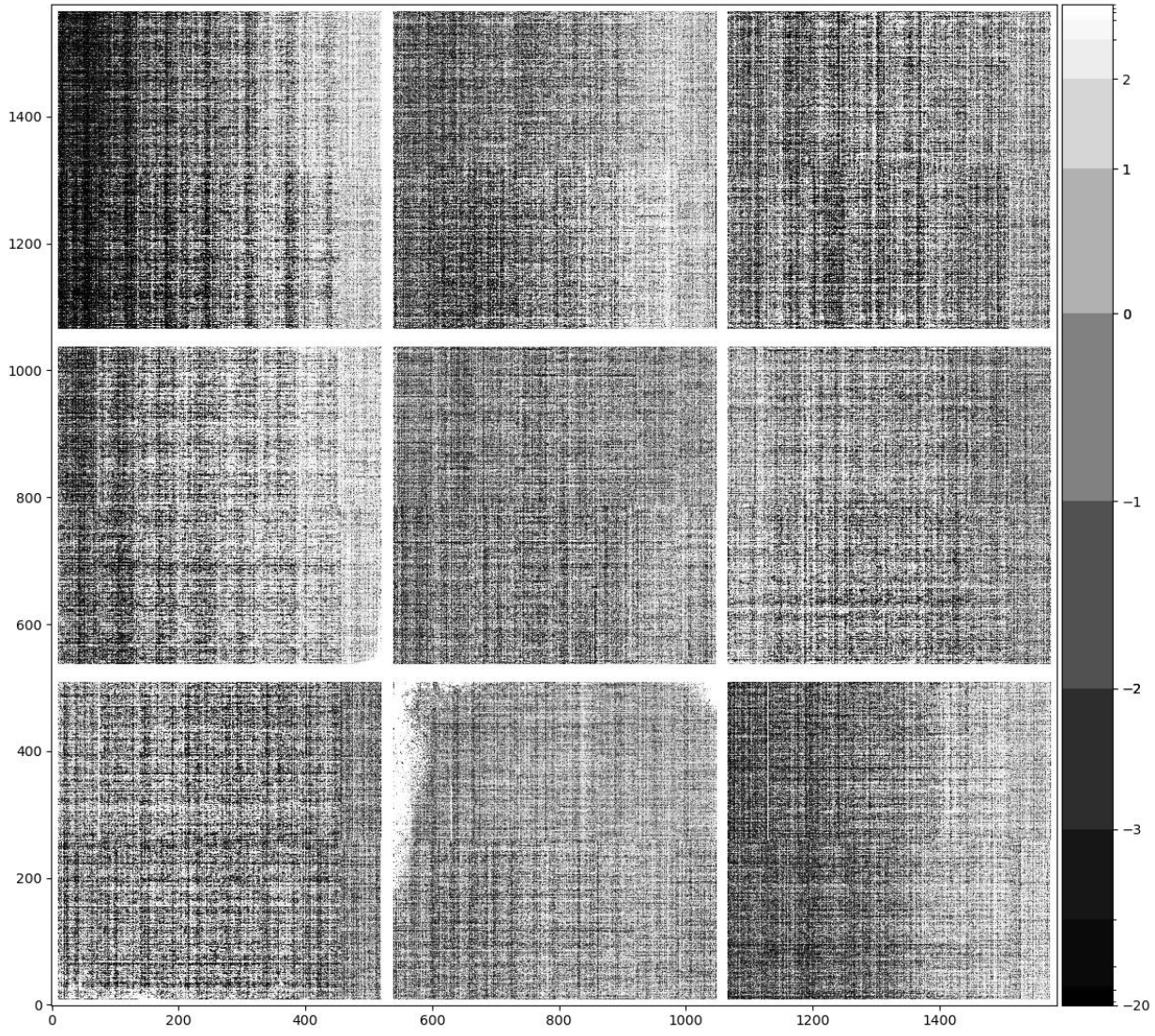

FIGURE 1: The phosphorescence seen in R22_S01, shown here in a dark exposure taken after a series of twilight flats (exposure=2024112000065). This material absorbs light at bluer wavelengths and re-emits that energy over a wide range of wavelengths.

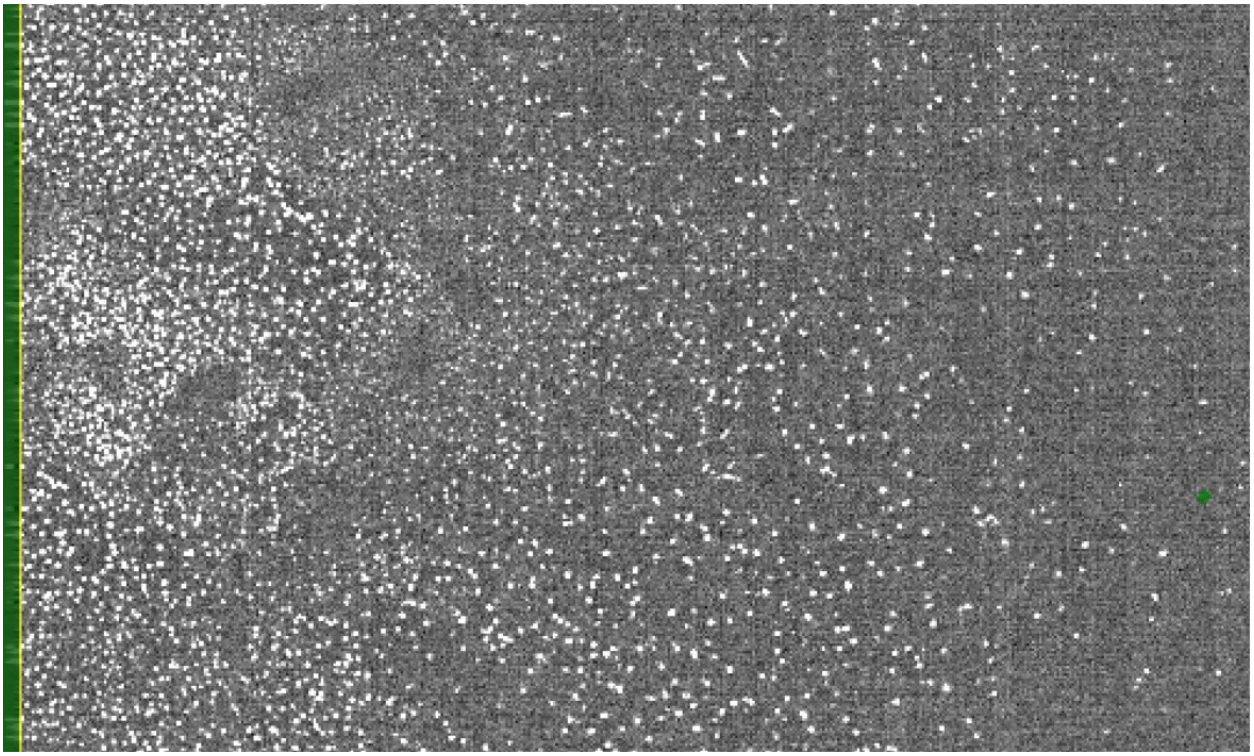

FIGURE 2: A full-resolution view of the edge of R22_S01. The features shown in this image are point-like sources caused by the trapped phosphorescence photo-resist.

flat quality during commissioning, we are finding that there is a sub-population that are not as severe, but likely have a similar physical mechanism. This population is still bright on the flat, with peaks around 1.2 (20% elevated relative to the flat), and may need to be masked as well. From an initial study in the lab, it appears that all ITL detectors on LSSTCam have a few of these kinds of defects, with two detectors approaching similar contamination levels as R22_S10 on LSSTComCam.

10.3 Saturated star effects

Although we expected to find saturated star trails coming from bright sources, the observed behavior of these trails is unique. Saturation spikes on most cameras appear as streaks extending from the core of the bright source along the direction of the parallel transfers, and truncate as the charge bleeds run out of charge (and can no longer overcome the potentials defining the pixel). The trails seem with LSSTComCam, however, extend the entire height of the detectors, crossing the midline break. These trails are also not at the expected high state, with the centers of these trails having flux levels lower than the average sky levels, creating dark trails. On the worst saturated objects, there is also evidence of charge pile-up near the serial readout, which can then create fan-like bright features at the edge of the detector. Those bright features can also then crosstalk onto other amplifiers.

The underlying physics is not well understood, and further study will be needed to see if we can correct these trails outside of the regions of charge buildup. Until we have a correction, we plan to begin masking both the trail and the fan-spread near the serial register.

Although we haven't seen identical features on LATISS, the presence of these odd trails on all LSSTComCam detectors suggests that this is a property of the ITL devices, and so will likely be seen on LSSTCam as well.

10.4 Gain ratios

LSSTComCam has been the first large-scale application of the updated "IsrTaskLSST" task, which uses a model of how the various signals combine to form the raw images to inform how we correct those signals during the ISR process. One improvement of this new task is that we now apply per-amplifier gains before flat correction, removing the gain component that was previously included in the flat correction. This results in the flat containing mainly

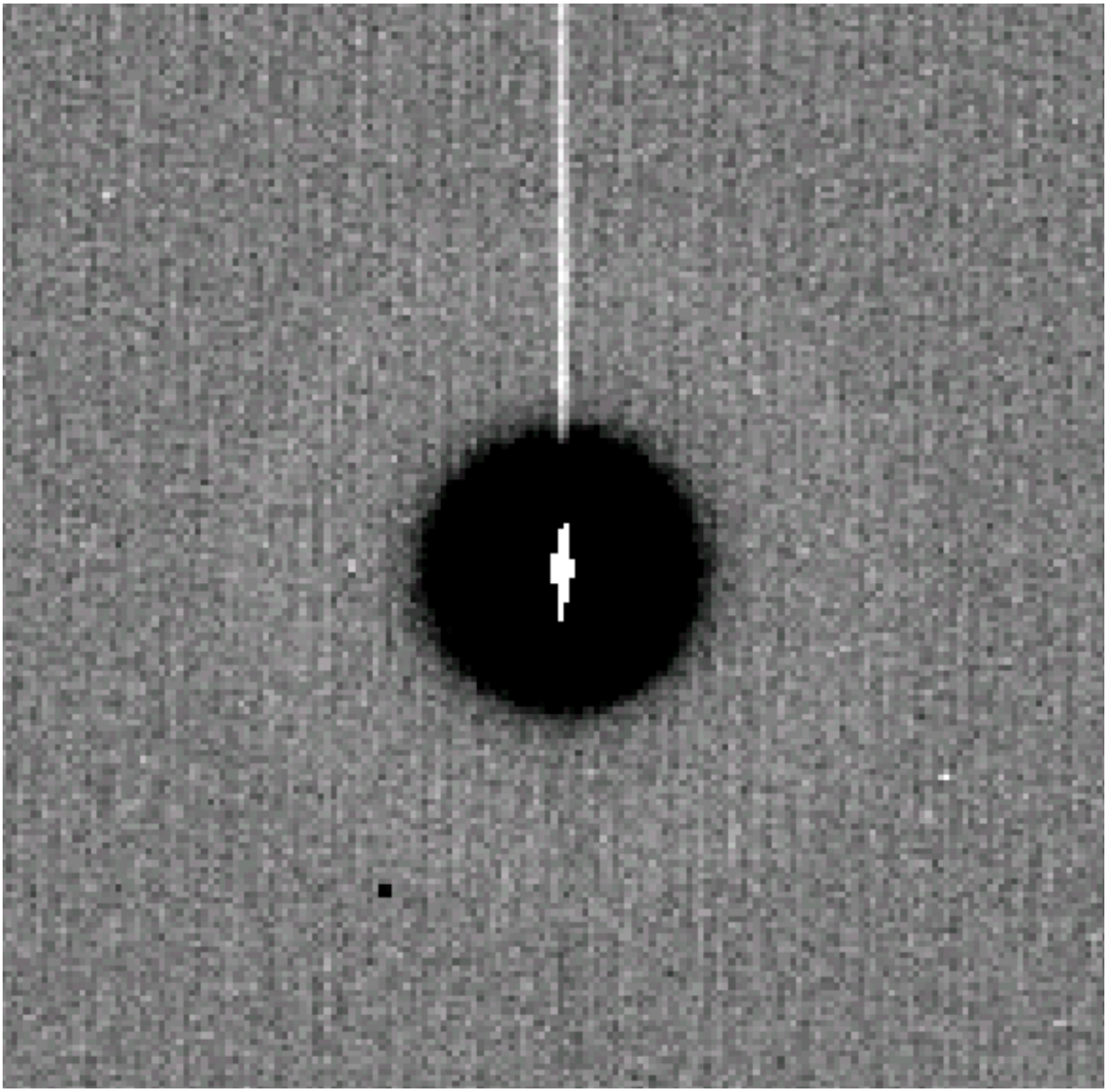

FIGURE 3: A close up of one of the largest vampire pixels. The bright core and region of depletion are clearly visible. Currently we only mask the core and depleted region, but will be extending this to mask the persistence-like trail that this feature leaves in the next few weeks.

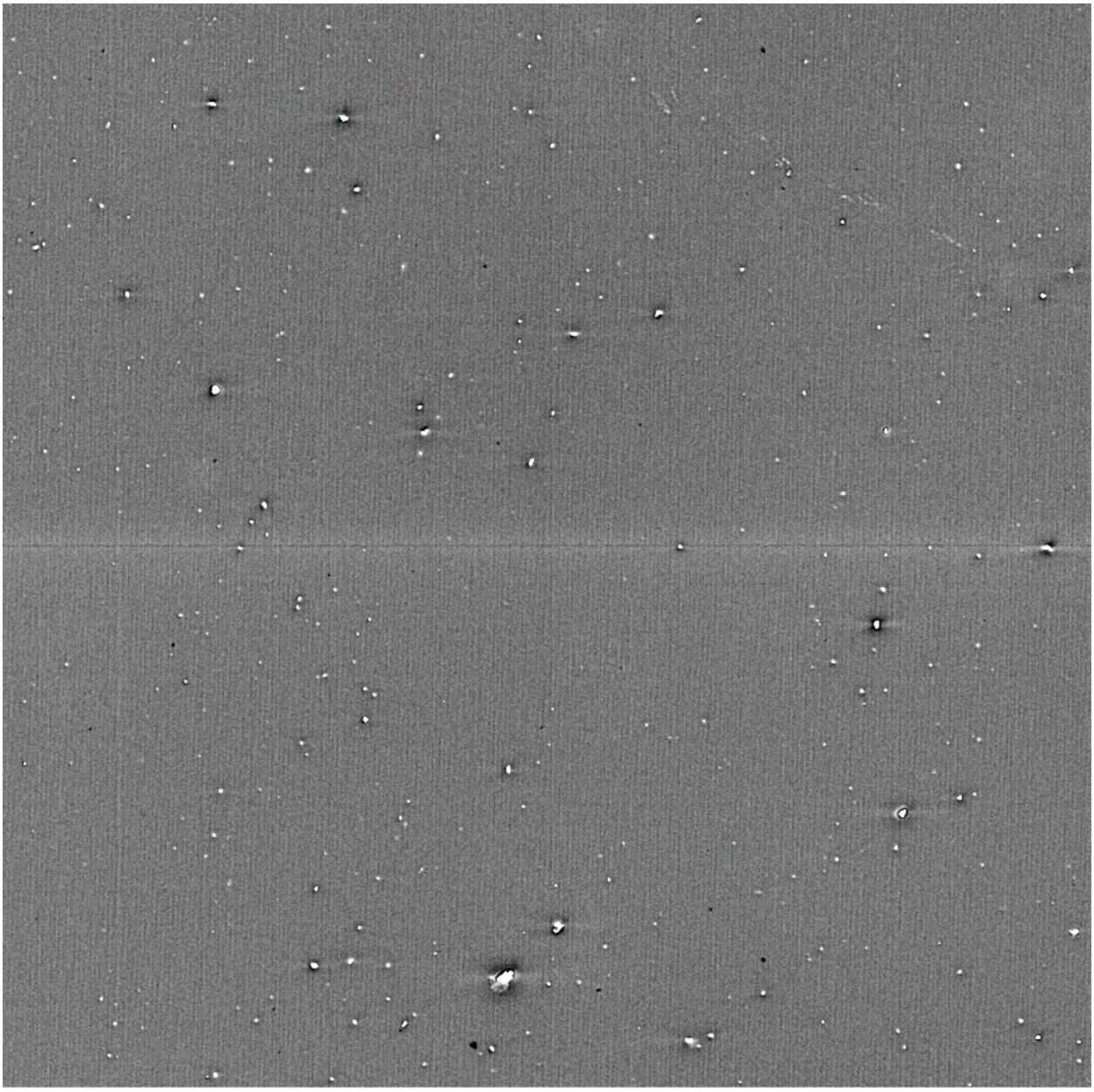

FIGURE 4: A view of detector R22_S10 in y-band, which has a large number of less significant vampire pixels.

QE and illumination patterns, which is much "flatter" than flats that also include gain terms (which offset the amplifiers relative to each other).

If we have properly diagonalized the flats and the gains, we would expect that applying the gain correction would create images with consistent sky levels across different amplifiers. However, when we look at images taken on-sky, our initial gain values result in some amplifiers being significantly different than their neighbors. The gains that we use are derived from the photon transfer curve (PTC), which uses flat pairs at different flux levels to monitor the properties of the noise. We have two of these sequences taken in the lab, and they disagree at the few percent level. This is similar in scale to the errors necessary to explain the on-sky differences. Further complicating this issue, the offsets seen in twilight data (used for flats) and that seen during the night also seem to differ. These differences so far have not been found to correlate with any device temperature, time, or voltage values. The gain correction fix appears to be stable, as we've only needed to generate and apply it once.

10.5 Crosstalk

We are currently using crosstalk values that were constructed by averaging the lab-based ITL measurements taken on LSSTCam. These are working better than expected, with residuals post correction being only a few electrons peak to peak. We plan to do a more complete crosstalk study using on-sky data, but the current results suggest that these lab measurements are sufficient for LSSTComCam, and expect the same to be true for LSSTCam.

10.6 Twilight flats

There is no flat screen currently available for the main telescope, and so we have constructed twilight flats for all bands using exposures taken to have median counts between 15000-20000 ADU. We have some dithering in the inputs, which have allowed us to reduce the impact of stars that print through into the flat. This reduction of non-sky signals is imperfect, and the current i-band flat shows a satellite trail as a result We are working to replace this flat using newly taken data.

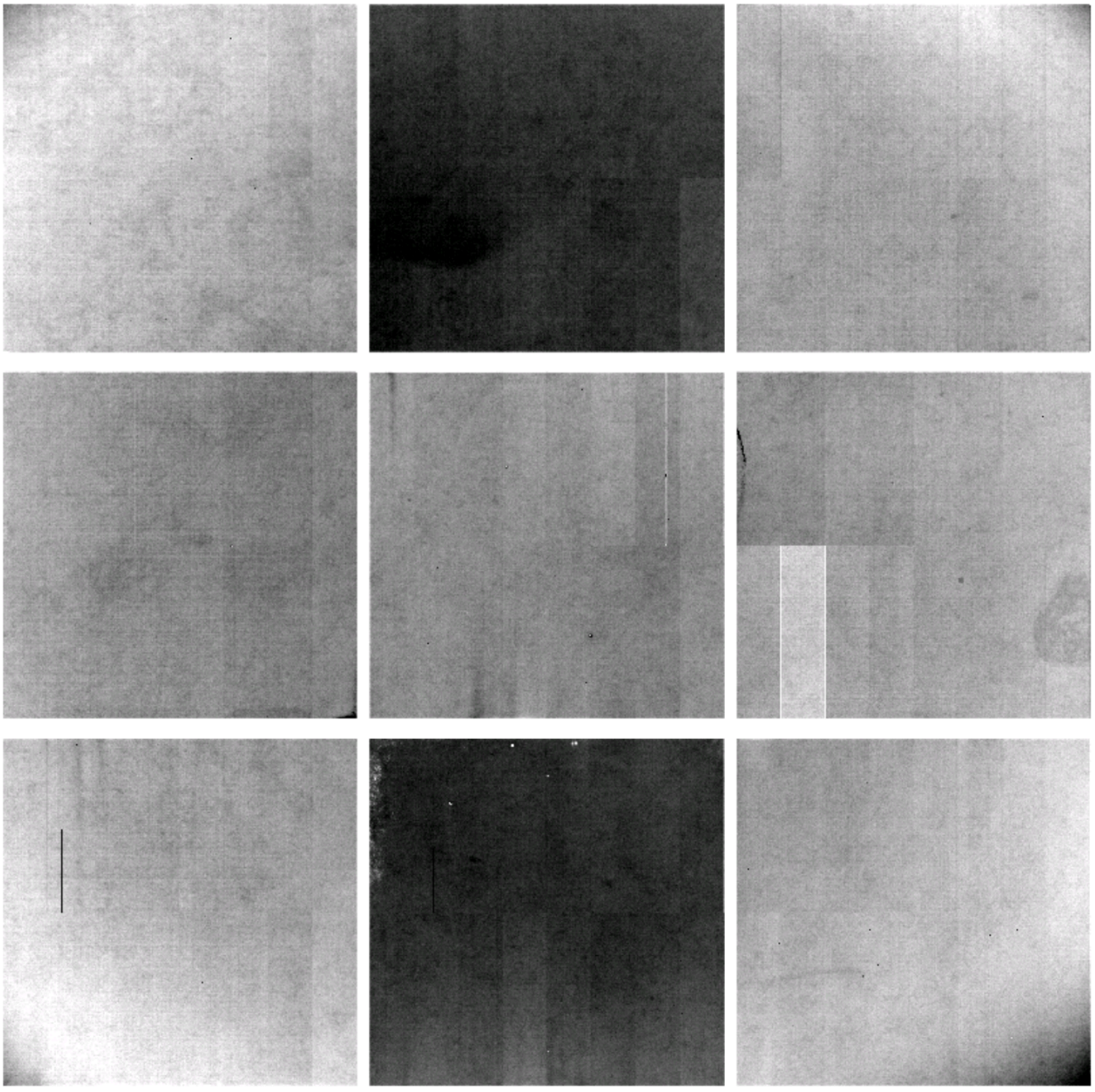

FIGURE 5: The ratio of the twilight-flat divided by a flat constructed from 94 r-band science frames. The scaling ranges from 0.9905 to 1.007. The visibility of amplifiers is caused by the unknown gain errors. The bottom right corner amplifier (C07) on R22_S21 is one of the indicator amplifiers, as it diverges from its neighbors. Although the C00-C03 amplifiers in R22_S12 also show significant offsets, these amplifiers also have an unrelated CTI issue, making them less reliable indicators.

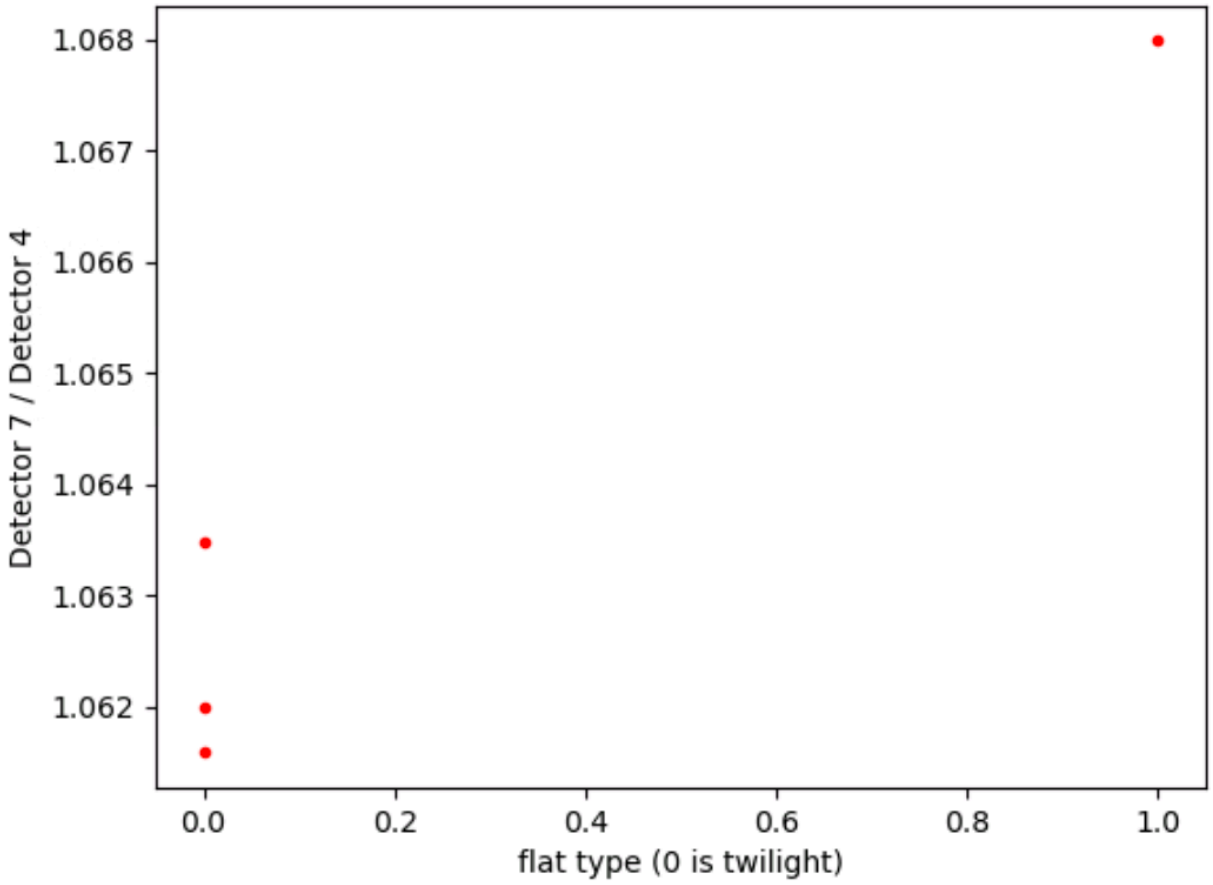

FIGURE 6: A comparison of the gain ratio between amplifiers in R22_S12. C07 is chosen as the indicator amplifier, and C04 is the reference. We have three twilight flat measurements taken at different rotator angles, and one from the 94 input sky flat.

10.7 Operations

The Telescope and Auxiliary Instrumentation Calibration Acceptance Board (TAXICAB) has been meeting previously to discuss LATISS calibrations, and has been helping manage calibrations for LSSTComCam. This process has not prevented problematic calibrations from being deployed (like the i-band flat with the satellite trail), but it has ensured that multiple people have checked some set of results. We are generating calibration verification reports regularly as part of this process (available at `https://s3df.slac.stanford.edu/people/czw/cpv_reports/`), and plan to add new metrics and checks to these as we discover more features of these detectors.

11 Low Surface Brightness

12 Astrometric Calibration

13 Photometric Calibration

14 Survey Performance

15 Sample Production

16 Difference Image Analysis: Transience and Variable Objects

16.1 DIA Status

As we have started to obtain repeated science-quality images of some fields, we have begun to build coadded templates as part of the regular weekly cumulative Data Release Processings. These mini-DRPs also include difference image analysis (DIA) of their constituent exposures. Using the DRP-produced templates, we have also obtained near-real-time difference images in Prompt Processing for a few exposures. We have not yet had the opportunity to begin tuning template generation, difference imaging, or Real/Bogus characterization of these data, so the report below provides an initial rough characterization of DIA performance.

16.2 ML Reliability and Artifact Rates

We ran a convolutional neural network on 51×51 difference, science, and template cutouts for 912k DIASources identified in the `w_2024_47` data release processing. This processing primarily includes data from extragalactic deep fields. These DiaSources were obtained from 4252 detector-visit images, implying an average of 21 DIASources per detector or about four thousand per equivalent full LSST focal plane. This is somewhat less than the ten thousand DIASources expected per visit and may reflect lower sensitivity due to ongoing image quality refinement and early templates.

The CNN was trained on simulated DC2 images with additional point source injection, so caution is needed when interpreting the values returned by this classifier on ComCam data. Nevertheless, Figure 7 shows a clear separation in reliability scores and would imply roughly a 3:1 bogus:real ratio if taken at face value. These values will be confirmed with manual inspection. We plan to train a purpose-built classifier on larger samples of labeled ComCam data.

17 Difference imaging QA

A difference imaging afterburner is run manually on Prompt Processing output to generate diagnostic plots, such as 8. From 8 we see the centroid of the PSF matching kernel sampled across one detector, which reveals a systematic offset between the science and template images. A similar offset is seen across the rest of the detectors for this visit, and in other visits. The images comprising the template used the same astrometric reference catalog as the science image in this case, but the template was constructed with the calibrate+characterizeImage pipeline while the science image was processed with calibrateImage. These are not included in the Prompt Processing payload to save critical time during observing.

The distribution of sources detected on the difference image reveals some detector-level effects that are not fully accounted for. Binning the locations of the diaSources in 1-D in 9 by their x- and y-values reveals systematic overdensities of detections at the amplifier boundaries in x (but not in y). Additional overdensities seen in y-band may be from the residual phosphorescent wax reported to be left on some chips beneath the AR coating.

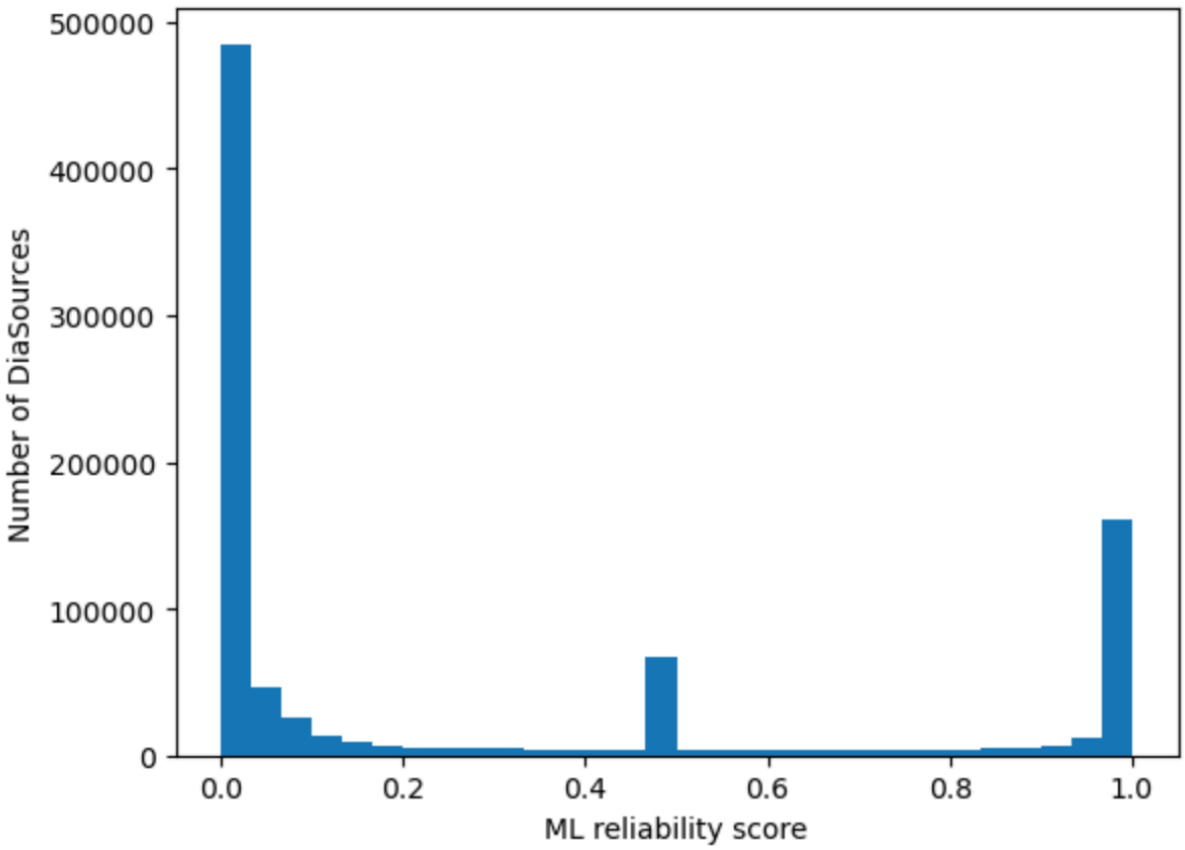

FIGURE 7: Histogram of machine-learned reliability scores computed on ComCam difference images.

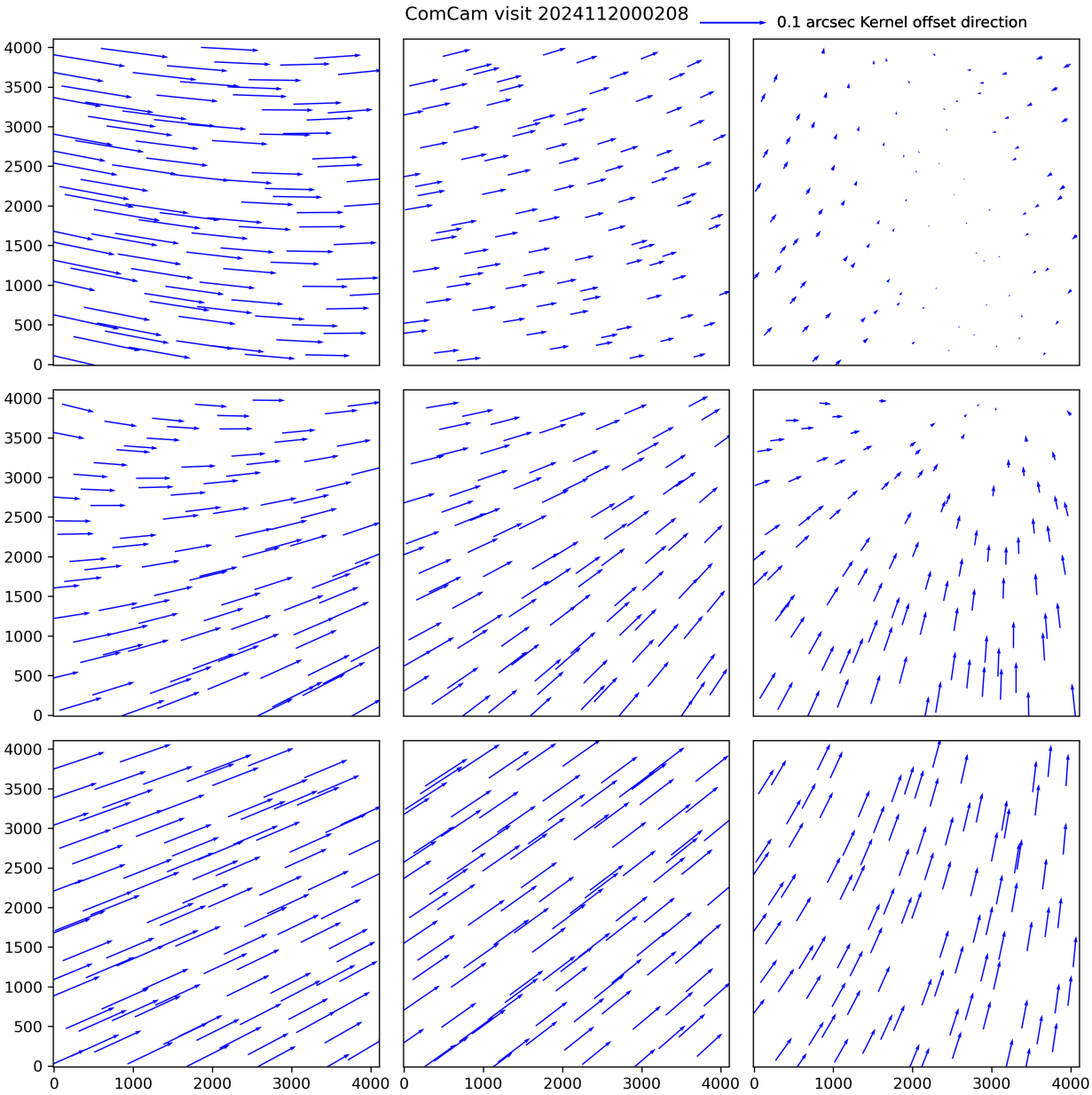

FIGURE 8: Quiver plot of the implied offset between the science and template images, calculated from the centroid of the PSF matching kernel. Note that the scale differs between the different panels, but that the overall pattern appears coherent over the focal plane, although each CCD was solved independently.

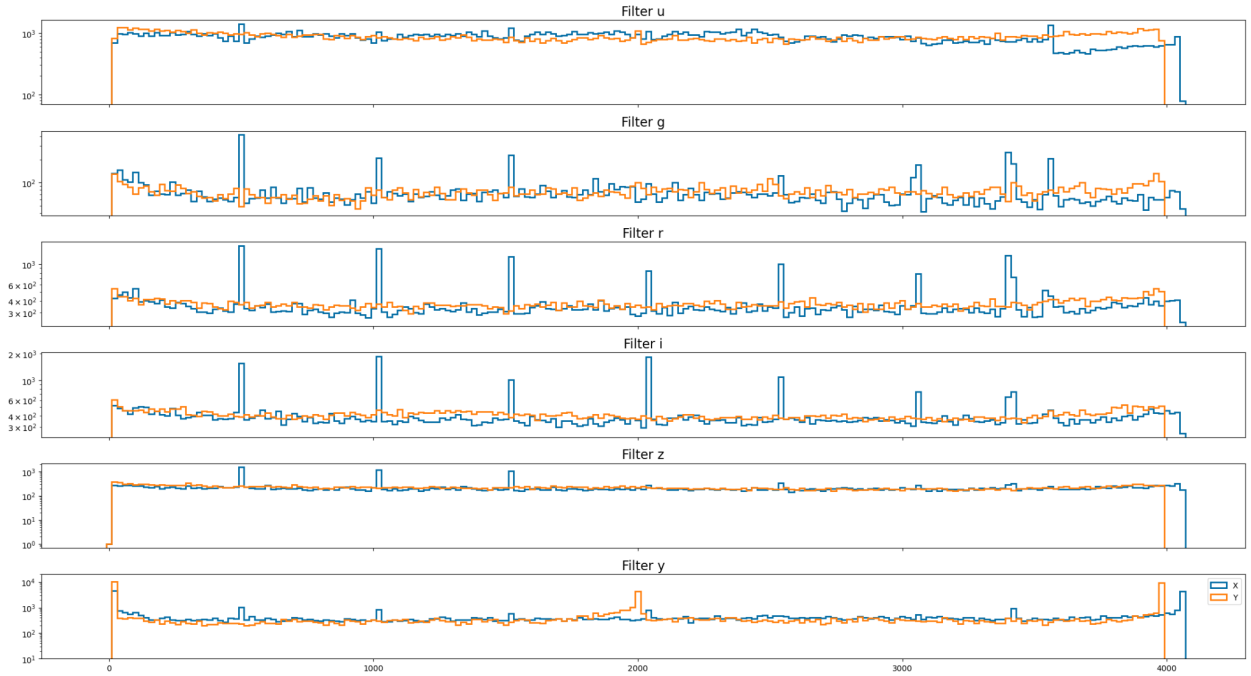

FIGURE 9: Binning the locations of the diaSources in 1-D by their x- and y-values reveals systematic overdensities of detections at the amplifier boundaries in x (but not in y).

17.1 Satellite Streaks

As orbital space becomes increasingly crowded, we expect to see many bright streaks, flares, and glints due to satellites and other reflective human-made objects orbiting the Earth. The majority of the population is in low-Earth orbit (LEO). For a review of the current status and likely impacts to LSST, please see `ls.st/satcon`.

As expected, many ComCam detector-visit images clearly show streaks. Visual inspection of nearly all ComCam images to date are being recorded on a best-effort basis in a Confluence Database dubbed "ComCam Satellite Spotter," and as of 2024 Nov 25 there are over 500 rows. The simple schema has one row per visit (if a streak crosses multiple detectors — which it often does — this is indicated in the "detector" column). In general, the morphology of streaks falls into one of these categories:

- Straight bright linear feature, typically at least 20 pixels wide, that crosses one or more detectors and goes off the edge (typical of most LEO satellites, such as Starlink)
- Shorter version of the above, with clear start and/or endpoints, which usually indicates

the object imaged is located at a higher-than-LEO orbital altitude (and/or the exposure integration time was unusually short)

- Intermittent linear feature, i.e., a dashed line, due to different parts of the satellite having different reflective properties
- A flare or glint brightening event that fades in and out along a linear trajectory, either isolated or as part of a longer streak
- Actually a bright star diffraction spike
- Actually a cosmic ray that was not repaired
- Variation of any of the above but in out-of-focus donut form (interestingly, depending on altitude, certain streaks may appear either in- or out-of-focus when stars appear as donuts)

Thanks to ComCam's relatively small field of view and the satellite population being as small as it ever will be during Rubin Commissioning and Operations, we have not yet seen an overwhelmingly bright satellite (e.g., BlueWalker 3 or one of the BlueBirds, all operated by AST SpaceMobile). Only a couple instances have streaks bright enough to induce visually-obvious crosstalk "secondary streaks;" the majority of streaks are relatively faint and the only portion of the image impacted are regions overlapping with the streak itself on the sky. Reliably determining streak width is an ongoing challenge, as it is not a delta function, and some of the brighter streaks do have notably extended stray light profile wings.

We note the Science Pipelines' algorithmic approach to identifying linear streak features (see `https://dmtn-197.lsst.io`) uses the detected mask plane and not the image array (pixel values) for efficiency. To more effectively detect faint streaks in difference images we have recently implemented a binning scheme designed to be sensitive to linear features that fall below the detection threshold.

17.1.1 Mitigating streaks in DRP

In most situations, the usual outlier clipping done during coadd assembly with the CompareWarp algorithm excludes streaks from coadds. The coadds where streaks remain all tend to have very few input images, so the streak was not able to be flagged and excluded as an out-

lier. Work is underway to assess the performance of detecting streaks via the kernel Hough transform in ComCam on top of the standard outlier clipping.

17.1.2 Mitigating streaks in AP

Work is underway to detect and masking streaks and glints in difference images. ComCam observations are an important data set for testing how well this works in various situations. A more detailed report will be available in the coming weeks. The efforts described here are distinct from work to identify long trailed sources and cross-check with an external satellite catalog.

17.2 Fake Source Injection for DIA

17.2.1 Selection of a data subset

In this subsection we select a portion of the observations processed by the DRP pipelines that include DIA, and run some simple analysis checks on the data contents. There are many fields being observed with LSSTComCam that span a large portion of the southern hemisphere accessible sky at this time of year (fall 2024).

From these, we make a selection, choosing a very well covered field in all bandpasses. In Fig.10 we show the full coverage of LSSTComCam up to current date.

In Fig 11 we apply a first cut on the observations, to narrow our visit list to a total of 24 visits. This cut involves a zenith distance of less than 45 degrees, as well as some technical parameters, derived from the nominal DRP DIA performance (ratio of PSF between template and science, as well as Kernel basis condition number).

We create a catalog of fakes for this sample of visits, by creating position and magnitudes of the synthetic sources to be injected. In Fig 12 we show the fake distribution per chip in our selection. We use sources that are possibly extended, and choose the fake location in its sourroundings. The magnitudes are chosen so they are within 1.5 magnitudes of the selected source host.

We run Alert Production pipeline with a set of additional tasks that handle fake injection on

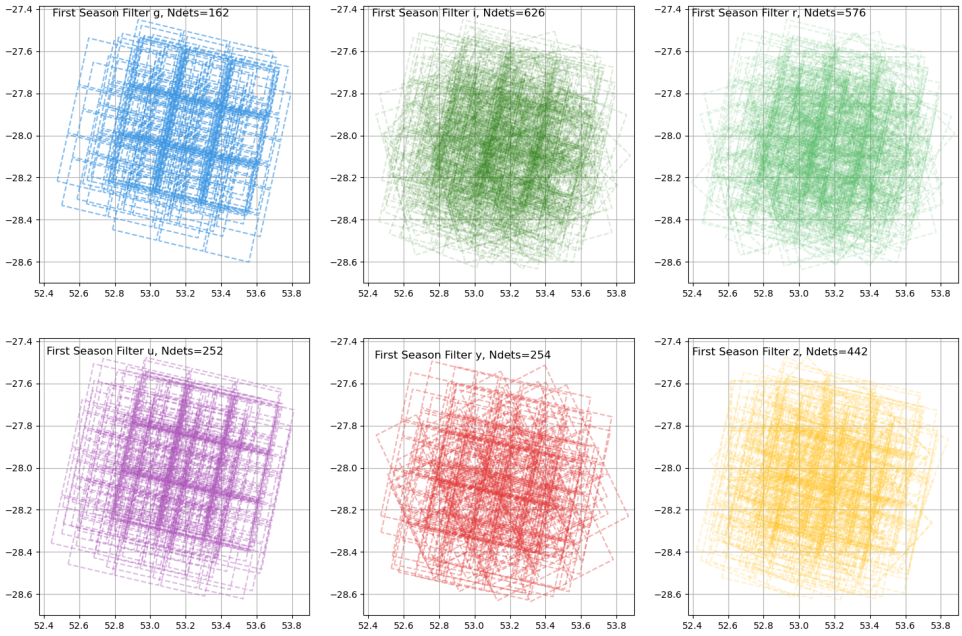

FIGURE 10: The full LSSTComCam set of observations overlapping the chosen field and with elevation > 45 above the horizon.

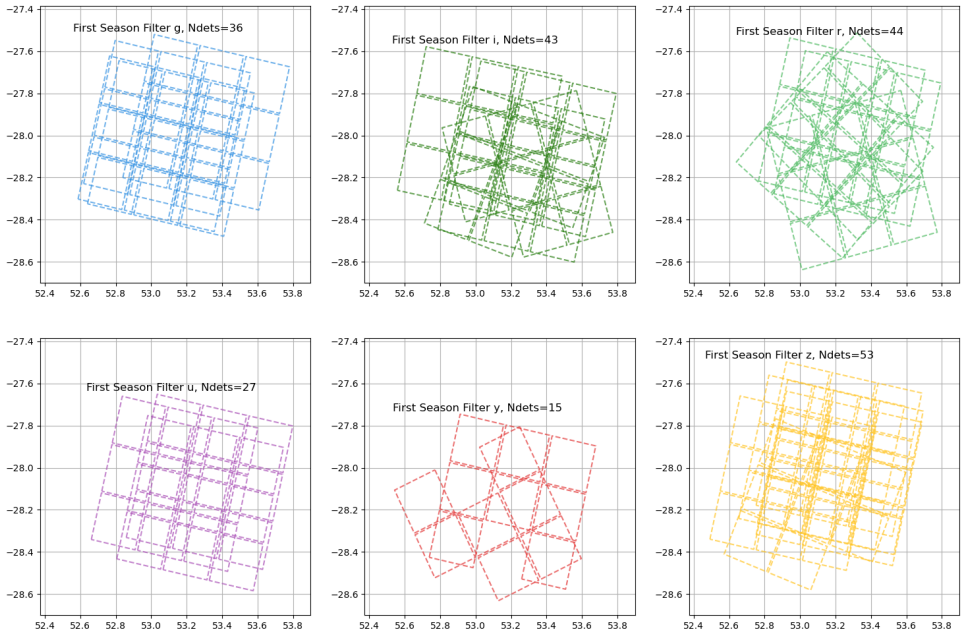

FIGURE 11: The selection of CCDs for fake injection processing.

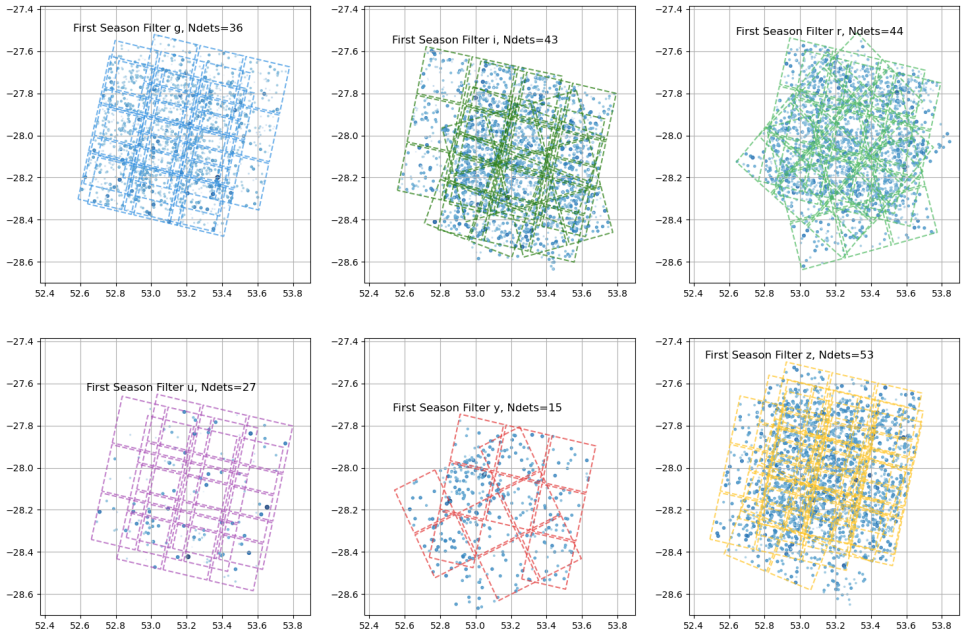

FIGURE 12: The fake position distribution in sky and in the CCDs footprint per bandpass.

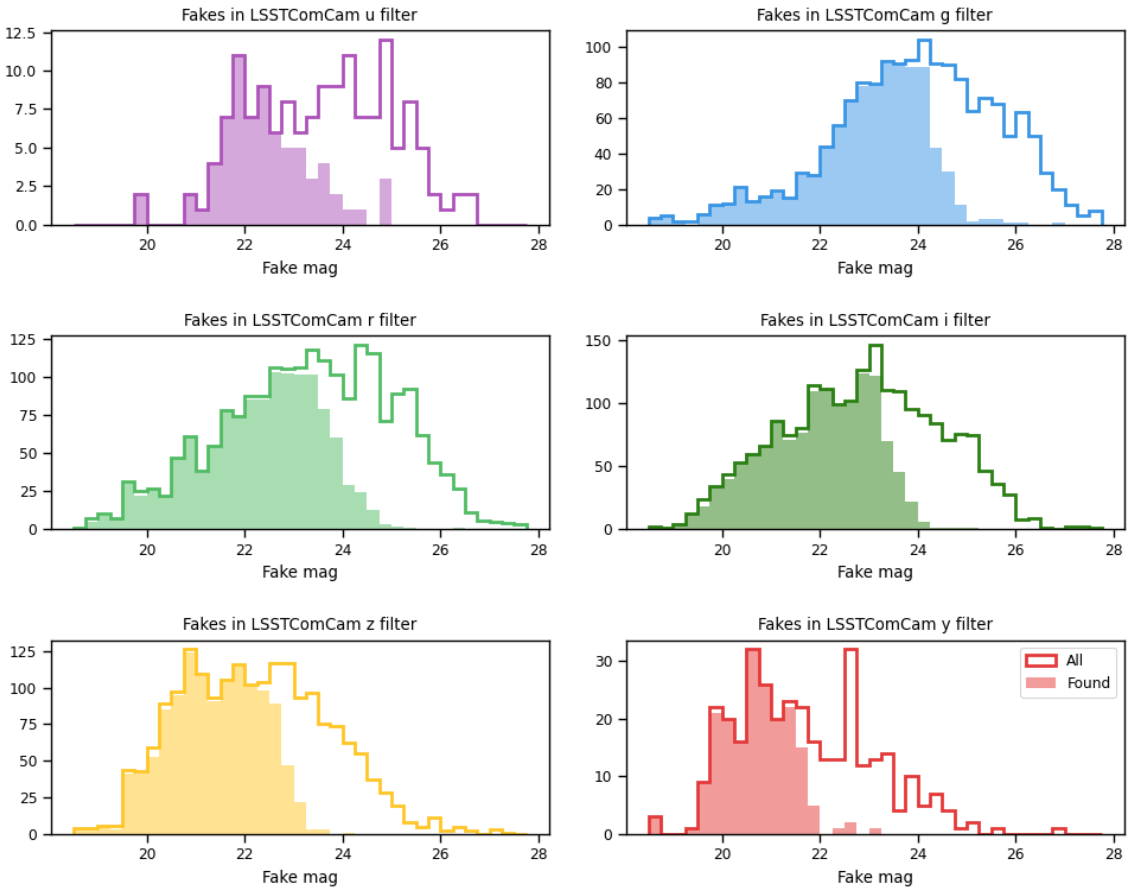

FIGURE 13: The distribution of magnitudes per bandpass for all the injected fakes (solid lines), and in shaded region the distribution of magnitudes of the fakes detected by the AP pipeline.

the *initial_pvi* images, and then the book-keeping tasks of fake catalog matching to diaSources as well as forced photometry for SNR estimation.

We then, can compile useful statistics about the fake source recovery, that informs us about DIA algorithm performance, as well as detection and measurement algorithm performance.

For this, we cross-match the position of our candidate detections, or *diaSources* with the positions of the synthetic sources, using a tolerance of $0.5''$ (roughly 2.5px).

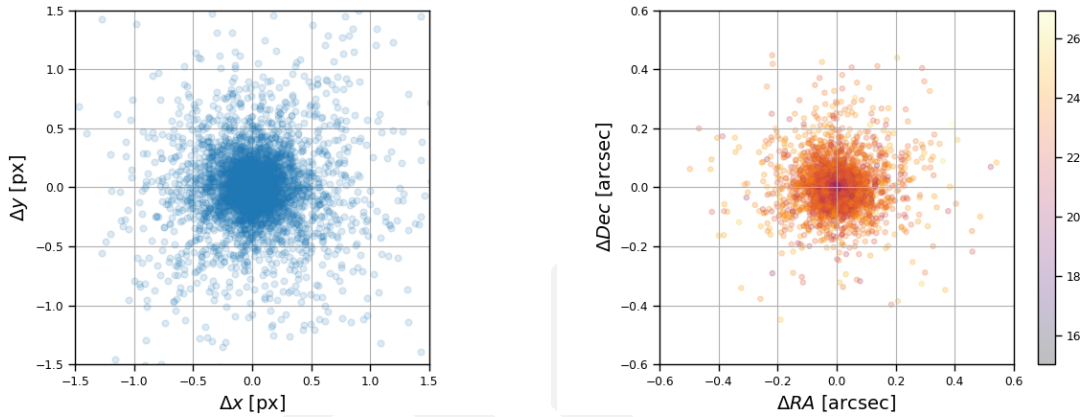

FIGURE 14: The scatter of the coordinate centroid recovery of the fakes. In the left we have the scatter around the true centroid in pixel coordinates, and in the right the scatter around the true center of fakes in sky coordinates (and in units of arc-seconds), wit the grid matching the pixel grid by means of the platescale. Also, we include the brightness in colormap.

Those fakes that found a match are called ”found fake” and objects that had no match we refer as ”lost” or ”missed” fakes. The rate of found to existing fakes is our recovery rate, Recall or Efficiency of detection.

18 Difference Image Analysis: Solar System Objects

19 Galaxy Photometry

20 Weak Lensing Shear

21 Crowded Stellar Fields

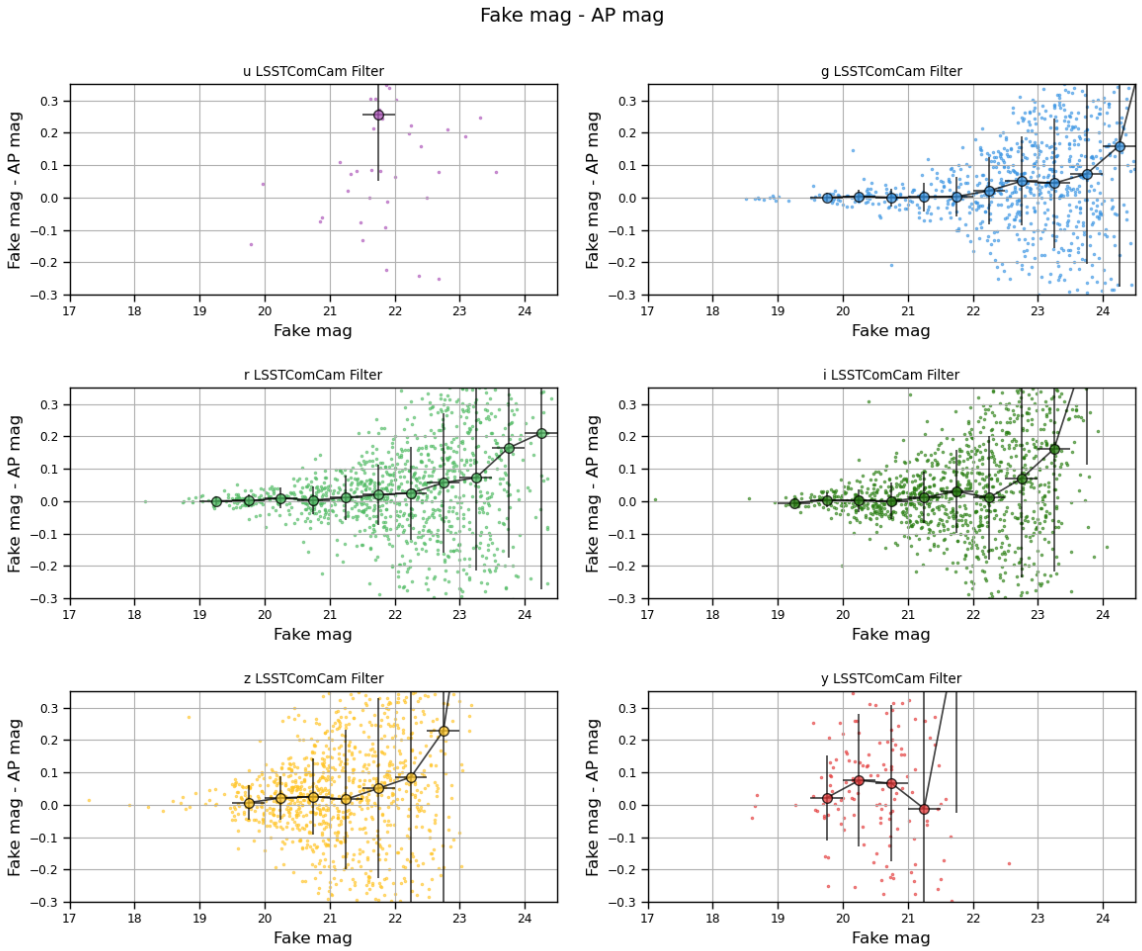

FIGURE 15: The recovered Aperture magnitude residual per filter for all the found fake sample, as a function of their true magnitude.

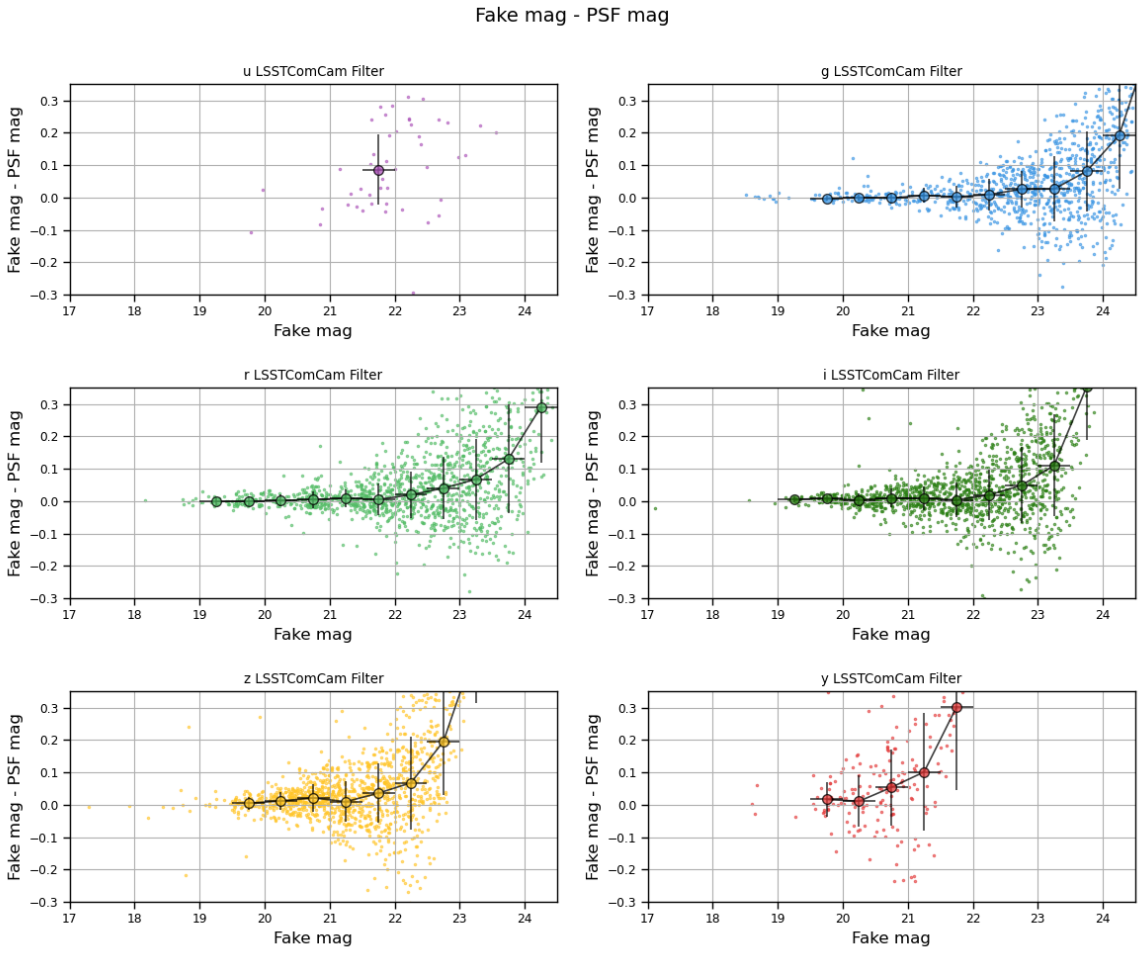

FIGURE 16: The residual of PSF magnitude measurement for found fakes, as function of their true magnitude.

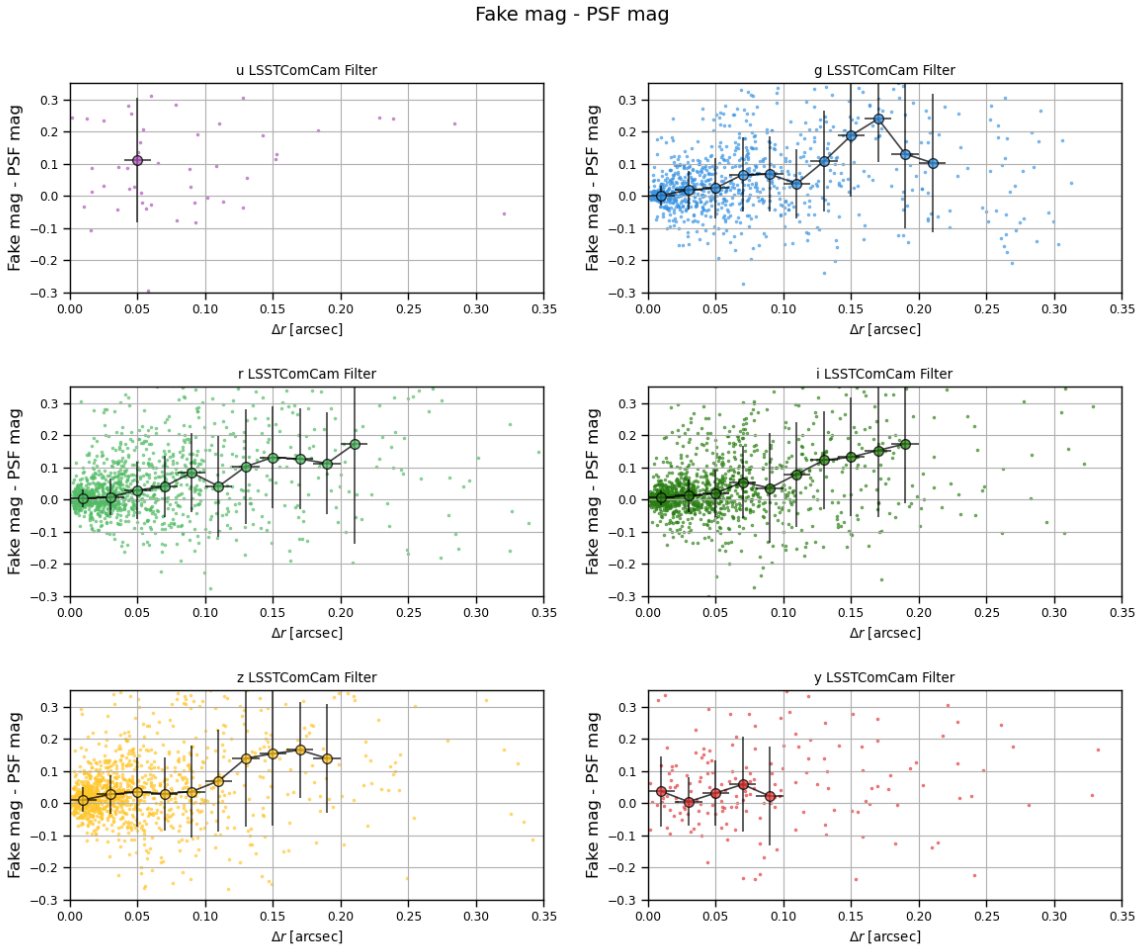

FIGURE 17: The PSF magnitude residual for the found fakes as function of their matching distance (in [arcsec]).

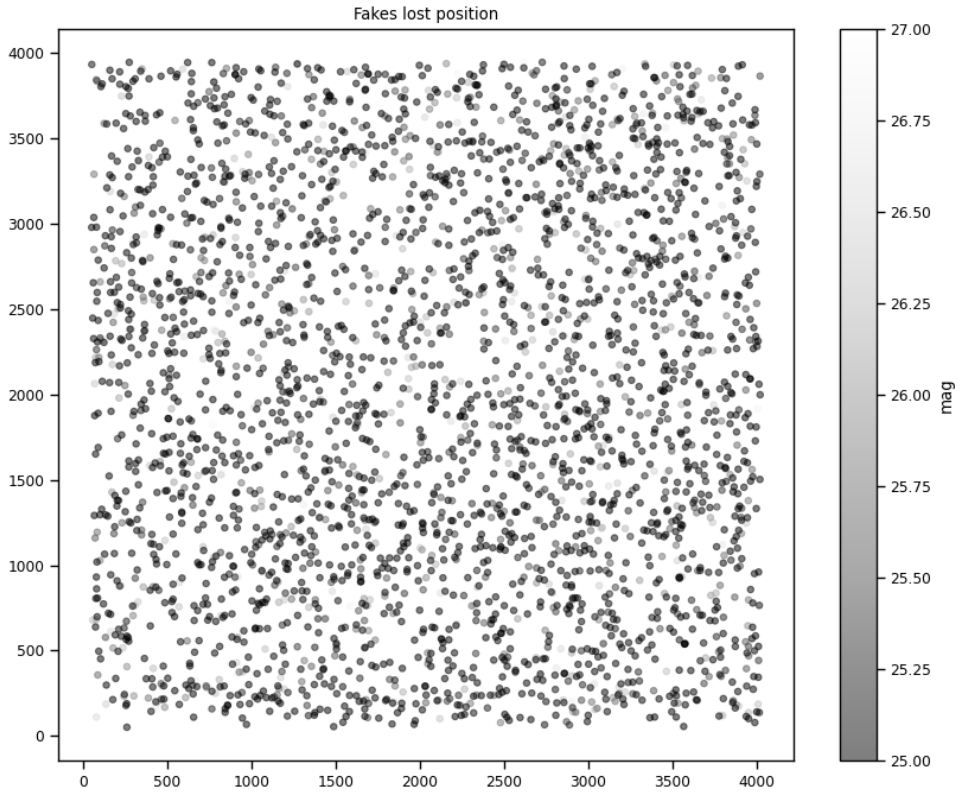

FIGURE 18: The scatter map of the lost sources in the detector coordinates. In gray scale in the colorbar we show the object magnitudes.

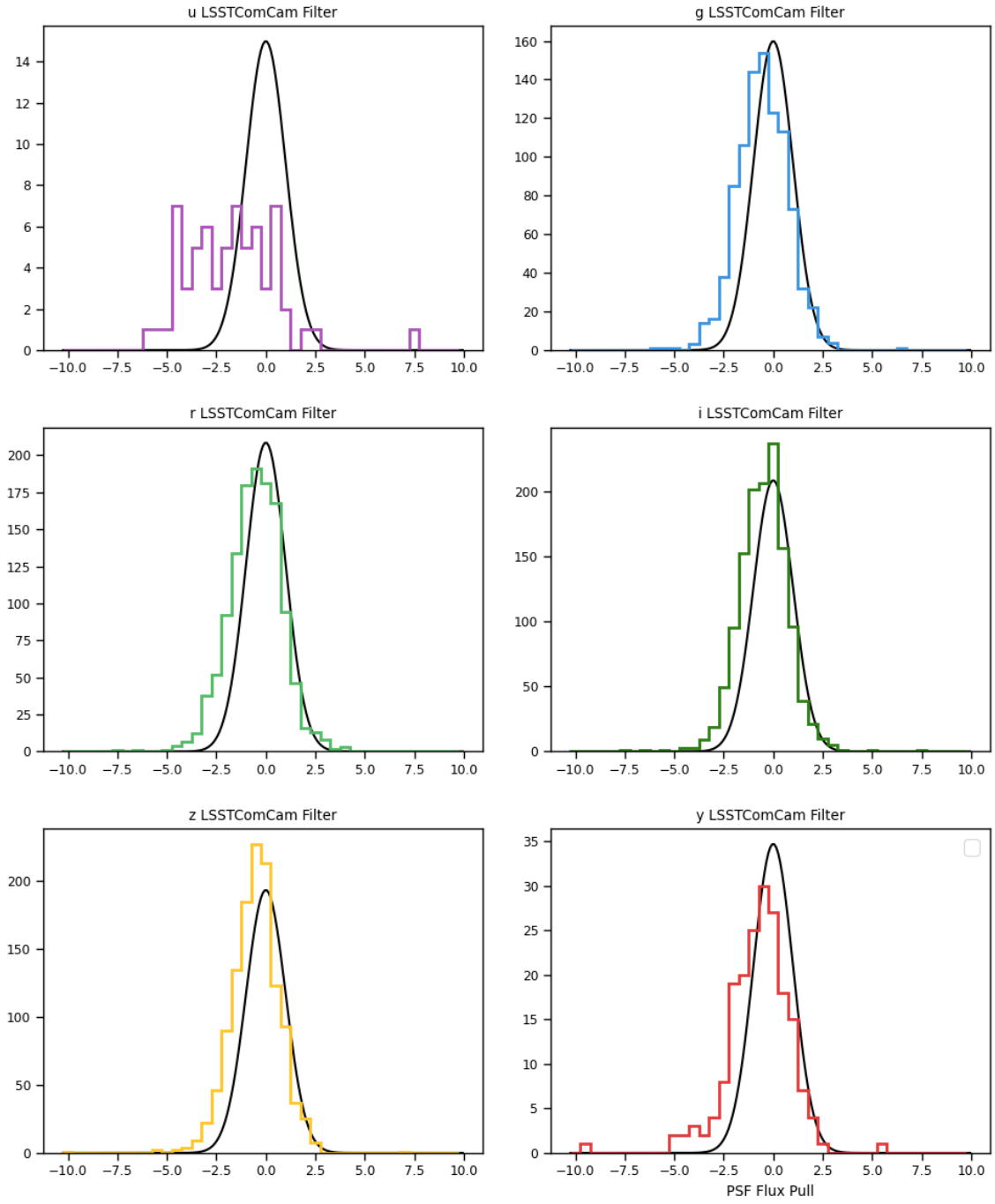

FIGURE 19: The flux pull distribution for all the found fakes, in each filter bandpass. A zero mean, unit dispersion Gaussian distribution function is also included for reference.

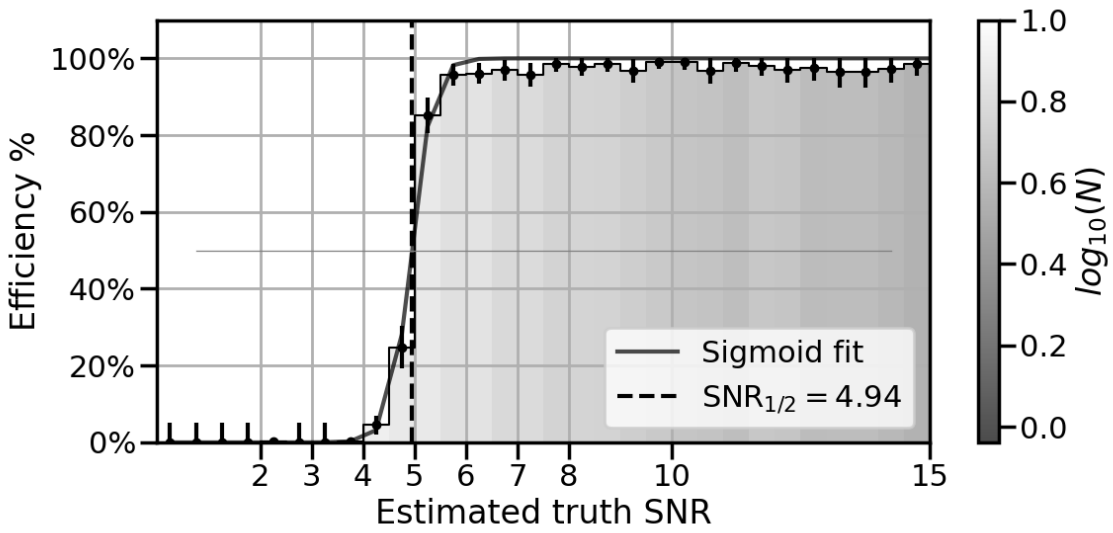

FIGURE 20: The detection efficiency as function of the PSF estimated S/N ratio of the fake sources. The SNR 1/2 parameter is also included in dashed lines, and represents the 50% efficiency S/N threshold value (lower is better).

22 Image Inspection

A References

[SITCOMTN-076], Bechtol, K., on behalf of the Rubin Observatory Project Science Team, S.R., 2024, Information Sharing during Commissioning, URL https://sitcomtn-076.lsst.io/, Vera C. Rubin Observatory Commissioning Technical Note SITCOMTN-076

[LSE-29], Claver, C.F., The LSST Systems Engineering Integrated Project Team, 2017, LSST System Requirements (LSR), URL https://ls.st/LSE-29, Vera C. Rubin Observatory LSE-29

[LSE-30], Claver, C.F., The LSST Systems Engineering Integrated Project Team, 2018, Observatory System Specifications (OSS), URL https://ls.st/LSE-30, Vera C. Rubin Observatory LSE-30

[RTN-011], Guy, L.P., Bechtol, K., Bellm, E., et al., 2024, Rubin Observatory Plans for an Early

Science Program, URL https://rtn-011.lsst.io/,
Vera C. Rubin Observatory Technical Note RTN-011

B Acronyms

Acronym	Description
ADU	Analogue-to-Digital Unit
CCD	Charge-Coupled Device
CNN	Convolutional Neural Network
DC2	Data Challenge 2 (DESC)
DIA	Difference Image Analysis
DRP	Data Release Production
ISR	Instrument Signal Removal
ITL	Imaging Technology Laboratory (UA)
LATISS	LSST Atmospheric Transmission Imager and Slitless Spectrograph
LSST	Legacy Survey of Space and Time (formerly Large Synoptic Survey Telescope)
ML	Machine Learning
PSF	Point Spread Function
QA	Quality Assurance
QE	quantum efficiency
RTN	Rubin Technical Note
SE	System Engineering